

## Effect of fluids on the $Q$ factors and resonance frequency of oscillating micrometer and nanometer scale beams

R. B. Bhiladvala\* and Z. J. Wang†

Cornell Center for Materials Research, Cornell University, Ithaca, New York 14853, USA

(Received 22 January 2003; revised manuscript received 30 October 2003)

Resonance oscillations of micrometer and nanometer scale beams in gases and liquids have increasingly important applications in physics and biology. In this work, we calculate fluid damping and its effect on damped resonance frequency  $\omega_d$ , and quality factor  $Q$ , for oscillating long beams at micrometer and submicrometer scales. For beams of nanometer scale, which are smaller than the mean free path of air molecules at standard conditions, the continuum limit breaks down and the commonly used Stokes drag calculation must be replaced by the appropriate calculation for rarefied gas flow. At scales where the continuum limit holds, this quasisteady Stokes solution is often still inapplicable due to the high resonant frequency associated with small beams, typically  $10^2$  MHz. The unsteady drag can be over two orders of magnitude higher than that predicted by the quasisteady Stokes solution and the added mass is nonnegligible. Here we calculate  $Q$  factors as a function of gas pressure over the range from  $10^{-5}$  torr to  $10^5$  torr, corresponding to free molecular to continuum limit. The comparison of the  $Q$  factors for two typical beams at various pressures suggests an advantage of using submicrometer scale over micrometer scale beams for applications near ambient pressure.

DOI: 10.1103/PhysRevE.69.0367XX

PACS number(s): 47.10.+g, 47.15.Gf, 47.45.-n, 81.07.-b

Oscillating beams at micrometer and submicrometer scales play at least two interesting roles. First, they offer simple systems for investigating scale effects of energy dissipation mechanisms both in the beam material [1,2] and as a result of interaction with their environment [2,3]. Second, their potential for applications such as atomic force microscopy in fluids, small biological mass detection via resonant frequency shift, and viscometry continues to grow. The resonance peak frequency ( $\omega_d$ ) and the  $Q$  factor ( $Q$ ), which allows measurement of dissipation through the sharpness of the resonant peak are the most widely used quantities in these applications.

The ambient gas pressure limit below which gas damping becomes negligible compared to damping within the material of the beam is of interest in many studies with small oscillators. Yasumura *et al.* [2] suggest a value of  $10^{-6}$  atm for this limit, while a different value is provided by Ho and Tai [4] ( $10^{-4}$ – $10^{-3}$  atm). In this paper we show that these disparate empirical thumbrules may be replaced by a calculation using beam properties and gas temperature and molecular weight as inputs.

Additionally, the requirement of working in vacuum often places an inconvenient constraint on many applications, such as small mass measurement through resonance frequency shift. This has been used for biological cell detection [5], which would be far more useful in either standard air or in liquid. The accuracy of measurement of the peak frequency shift depends on the  $Q$  factor of the beam. Recent experiments of Sekaric *et al.* [6] use laser-light driving to overcome fluid damping losses in a paddle-beam structure oscil-

lating in air at atmospheric pressure [6]. Quantification of fluid effects at scales relevant to these applications has focused strongly on continuum flows [3,7,8]. In this paper we present a framework which enables simple calculations with either a continuum or noncontinuum approach, as appropriate to the problem. Calculations for beams of submicrometer and  $10\ \mu\text{m}$  width suggest a surprising advantage of the use of submicrometer scale beams over larger beams in air near atmospheric pressure.

Two aspects are worth noting as the beam approaches submicrometer scale. First, the continuum limit can break down even at atmospheric pressure, as seen in Fig. 1. Thus the usual quasisteady Stokes drag estimate needs to be replaced by rarefied gas flow results. Second, these beams typically have a high frequency, on the order of  $10^2$  MHz, with stronger unsteady effects. Unsteady effects have two mani-

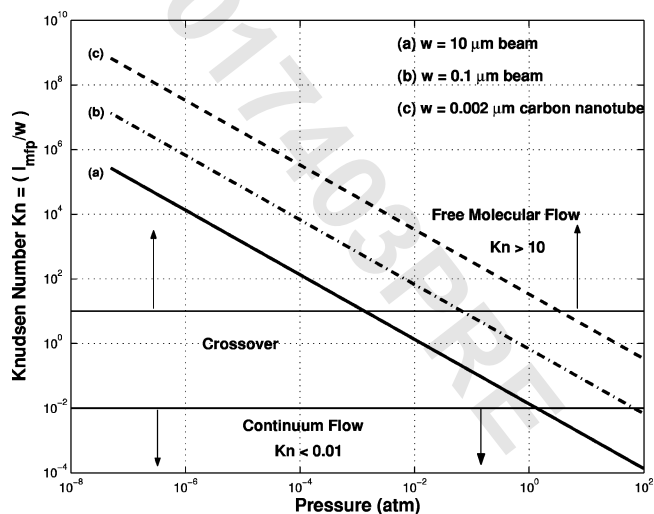


FIG. 1. Continuum, free molecular, and crossover flow regimes as a function of beam size and pressure in dry nitrogen at room temperature (300 K).

\*Also at Applied and Engineering Physics, Cornell University.

†Also at Theoretical and Applied Mechanics, Cornell University. Electronic address: rustom.bhiladvala@cornell.edu, jane.wang@cornell.edu

festations: (1) the presence of an added mass associated with the force to accelerate surrounding fluid, and (2) a frequency dependence of the damping coefficient. In this paper, we study fluid damping and its consequence on  $Q$  factor in both the molecular and the unsteady continuum limit. To do so, we first relate  $Q$  for the beam in a fluid to the  $Q$  value in vacuum.

The  $Q$  factor for a linear harmonic oscillator with mass  $M$ , stiffness  $K$  ( $\omega_0 = \sqrt{K/M}$ ), and damping  $C$ , defined in terms of average energy stored and dissipated per cycle, may be written as

$$Q = 2\pi \frac{E_{\text{stored}}}{E_{\text{diss}}} = \frac{K + M\omega^2}{2C\omega} = \frac{Q_p^2 - \frac{1}{4}}{\sqrt{Q_p^2 - \frac{1}{2}}}, \quad (1)$$

where  $Q_p = \sqrt{MK}/C$  is a property-dependent, dimensionless factor. The expression in terms of  $Q_p$  is obtained by evaluating  $Q$  for beam oscillation frequency  $\omega$  equal to the damped resonance peak frequency,

$$\omega_d = \left[ \frac{K}{M} \left( 1 - \frac{C^2}{2MK} \right) \right]^{1/2} = \omega_0 \left[ 1 - \frac{1}{2Q_p^2} \right]^{1/2}. \quad (2)$$

When  $Q_p \gg 1$ ,  $Q$  reduces to  $Q_p$  and  $\omega_d$  to  $\omega_0$ . However, if the damping is significant, even when the motion remains harmonic,  $\omega_d$  will be significantly different from the natural frequency in vacuum and iteration between Eq. (2) and the calculation below for fluid damping is required. To include damping forces due to ambient fluid we define total damping  $C = C_s + C_f$ , where the subscripts  $s, f$  denote structural (solid) and fluid quantities respectively. In some regimes of flow, the force on the beam due to the fluid, opposing the motion, in phase with the acceleration, is significant. This may be represented by an added mass  $M_f$  and the oscillating beam may be considered to have an effective mass  $M = M_s + M_f$ .

From Ref. [1], the undamped resonance frequency of a beam of length  $l$ , width  $w$  (normal to oscillation), and thickness  $t$ , in the absence of fluid added mass, is given by

$$\omega_0 = \sqrt{\frac{K_s}{M_s}} = (C_1)^2 \sqrt{\frac{EI}{M_s l^3}} = (C_1)^2 \sqrt{\frac{E}{12\rho_s l^2}} t, \quad (3)$$

where  $K_s$ ,  $\rho_s$ ,  $E$ , and  $I$  are the effective stiffness, density, Young's modulus, and cross-sectional moment of inertia of the solid beam.  $C_1$  is 1.88 for cantilever beams and 4.73 for doubly clamped beams vibrating in the fundamental mode. If the effective stiffness  $K$  in the fluid remains unchanged from its value in vacuum  $K_s$ , given by Eq. (3), substituting for effective  $M$ ,  $K$ , and  $C$  in  $Q_p$ , we obtain,

$$Q_p = \left[ C_1^2 \left( \frac{E\rho_s}{12} \right)^{1/2} \frac{wt^2}{l} \right] \left[ \frac{1}{C_s} \right] \left[ \frac{[1 + (M_f/M_s)]^{1/2}}{1 + (C_f/C_s)} \right]. \quad (4)$$

Terms in the third set of large square brackets yield the modification of  $Q_p$  due to fluid added mass and damping and have value 1 in vacuum. Terms in the first set of large square brackets show that the scaling dependencies of  $Q_p$  on geometry and properties,  $w^1, t^2, l^{-1}, (E\rho_s)^{1/2}$  accrue from beam solid mass and stiffness alone, which is useful in determining the scaling properties of the structural damping coefficient  $C_s$  from measured  $Q_p$  in vacuum.

We now move to the task of determining fluid related effects, specifically the values for damping  $C_f$  and added mass  $M_f$ , where it is relevant. Operation of beam oscillators in a gaseous environment, at low pressures or with nanoscale beams at atmospheric pressure may give rise to situations where the mean free path of gas molecules is not small compared to beam size. In this case, the molecule number density and properties such as density and viscosity computed from it will show large, discontinuous fluctuations about their mean values; solutions of the Navier-Stokes equation which consider the fluid as a continuum are no longer valid. With decreasing beam size, the departure from continuum increases and the fluid moves to the regime of free molecular flow. In this regime, a large mean free path with respect to beam size and distance from walls implies that molecules which suffer a collision with the beam are unlikely to suffer a second collision with it. The velocity distribution function of molecules seen by the beam will therefore remain unchanged as a result of the motion of the beam and allows for a simpler computation of force on the beam.

For gases, determining the regime of flow is clearly the first step in calculating fluid forces on the beam. To do so, we compute the mean free path ( $l_{mfp}$ ). For a dilute gas with molecules modeled as hard spheres of a single diameter  $d$ , the scattering cross section  $\sigma = \pi d^2$  [9], the mean free path scales inversely with  $\sigma$  and number density  $n$ :

$$l_{mfp} = \frac{1}{\sqrt{2}\sigma n} = 0.23 \frac{K_B T}{d^2 P}, \quad (5)$$

where  $K_B$  is the Boltzmann constant,  $T$  and  $P$  the absolute temperature and pressure, respectively. With  $d \approx 0.37$  nm, for air at standard temperature and pressure,  $l_{mfp} \approx 65$  nm.

The Knudsen number  $\text{Kn}$  measures the ratio of the mean free path of gas molecules to the size of the beam. For long beams, we note that the appropriate measure of beam size for fluid interaction is  $w$ , the transverse dimension normal to the direction of motion, hence  $\text{Kn} = l_{mfp}/w$ . The undamped resonance frequency, however, varies linearly with thickness  $t$  and is independent of  $w$ , hence we may specify the beam using  $l, w, t$  or  $l, w, \omega_0$ .

For air under isothermal conditions, the flow is in the continuum regime for  $\text{Kn} \leq 0.01$ , in the free molecular regime for  $\text{Kn} > 10$ ;  $0.01 \leq \text{Kn} \leq 10$  defines a crossover regime where neither continuum nor free molecular flow adequately describe gas behavior [10]. Figure 1 shows the flow regimes for beams of three widths, 10  $\mu\text{m}$ , 100 nm, and 2 nm. The 2 nm carbon nanotube would be in the free molecular regime up to pressures of 1 atm. Like the 100 nm beam, a continuum Navier-Stokes solution is inappropriate for it even at

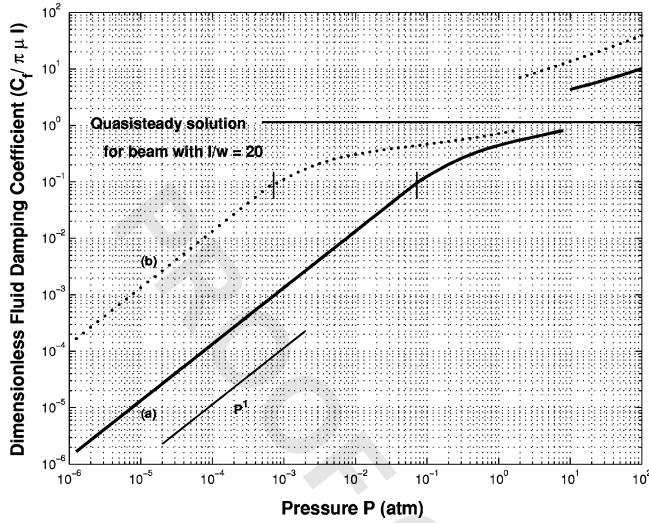


FIG. 2. Nondimensional gas damping coefficient, computed for dry  $N_2$  at 300 K for beams with (a)  $w=100$  nm, 530 MHz frequency, (b)  $w=10$   $\mu\text{m}$ , 1 MHz frequency and aspect ratio  $l/w=20$ . Short vertical lines on each curve mark the change from the free molecular solution (damping varies linearly with pressure) to the steady Boltzmann-BGK crossover solution, which underpredicts unsteady damping and shows a jump at the continuum limit. Temperature and molecular weight of the gas are the only other inputs.

pressures in tens of atmospheres. The largest 10  $\mu\text{m}$  beam will begin to show continuum behavior at pressures above 1 atm.

In the continuum regime, the fluid density  $\rho_f = mn$ , where  $m$  is the mass of one molecule. For dilute gases, from kinetic theory, the dynamic viscosity is

$$\mu = 0.45mnU_{th}l_{mfp}. \quad (6)$$

Here  $U_{th} = \sqrt{3K_BNT/M_m}$  is the root mean square value from the Maxwellian distribution for molecular velocity,  $N$  is Avogadro's number, and  $M_m$  is the molecular weight in kg/mol (e.g., 0.028 for  $N_2$ ). The coefficient 0.45, from Ref. [10], is obtained using a hard sphere molecular model for interactions and yields values in close agreement with those tabulated from experiment for common gases at atmospheric pressure. Since  $l_{mfp}$  is inversely proportional to density  $n$ , the dynamic viscosity is independent of fluid density. For consistency, we will use  $\mu$ , calculated by Eq. (6), as a parameter for presenting  $C_f$  in nondimensional form in all the flow regimes as shown in Fig. 2.

We first derive the force on the beam in the free molecular limit. Assuming that all the molecules are specularly reflected, the drag force  $F_d$  is caused by the difference in momentum exchange of the gas molecules striking the front and back of the moving beam. A simplified calculation for a plane of length  $l$ , width  $w$ , and molecular velocity  $U_{th}$  along the direction of motion of the beam yields

$$C_f = \frac{F_d}{u} = 2 mnU_{th}lw. \quad (7)$$

A more exhaustive treatment for a beam of cylindrical geometry, valid for nonspecular reflection and arbitrary Mach

number, may be found in Ref. [11]. After evaluation of four integrals at vanishingly small Mach numbers, this solution yields Eq. (7), with a nearly identical constant (2.03). Damping coefficients for two beams as a function of pressure in this regime, plotted in Fig. 2, are 2–5 orders of magnitude lower than the quasisteady continuum solution.

In the crossover regime between free molecular and continuum flow, the velocity distribution function of molecules interacting with the beam begins to show a deviation due to previous interactions with it. In this regime, we use a solution of the Boltzmann equation with the BGK model, which employs a simplified collision operator with a single time scale. From this solution for flow past a cylinder [12], we obtain a value for the damping coefficient,

$$C_f = \frac{F_d}{u} = mnU_{th}lw \left[ \frac{\pi^{3/2}Kn}{\alpha} \right], \quad (8)$$

$$\alpha = \ln \left( \frac{2\sqrt{\pi}Kn}{S} \right) - \gamma + \frac{1}{2} + \Lambda \sqrt{\pi}Kn, \quad (9)$$

where  $S$ , the Mach number, is the ratio of beam velocity to the molecular velocity and  $\gamma$  is the Euler constant = 0.5772. In this regime, the assumption that all molecules are specularly reflected is incorrect.  $\Lambda$ , dependent on the slip velocity, varies between 1 and 1.5 in the Knudsen number range 0.01–50. We note that the tabular values for  $\Lambda$  in Ref. [12] can be approximated to within 2% rms (and 4% maximum) error, by

$$\Lambda = 1 + \frac{1}{2}(1 - e^{-Kn/2}). \quad (10)$$

The crossover solution [12] is valid for low Mach number  $S$ . If the Mach number is not low enough,  $\alpha$  in Eq. (8) becomes zero, then negative, leading to large unphysical values for  $C_f$ . The low Mach number requirement effectively restricts use of this solution to values of  $Kn$  such that  $\alpha \geq 3$ . In the high Knudsen number limit, the expression in parentheses in Eq. (8) tends to a constant value close to 2, in accord with the free molecular solution, Eq. (7). At the low end of the crossover regime, approaching continuum flow, the expression yields values almost equal to  $Kn$ . This solution for damping  $C_f$  is plotted in Fig. 2.

We now consider the case when the continuum limit for fluid flow around the oscillating beam holds, as for liquids and for gases when the mean free path of molecules is much less than the diameter of the beam. Stokes' familiar quasisteady solution is frequently used for a quick estimate. For small oscillating beams, such an estimate can be over two orders of magnitude too low, when compared to experiments [7] and to calculations using a solution which correctly accounts for the frequency dependence, as presented in recent work (e.g., Refs. [3,7]).

Two relevant dimensionless parameters arise for unsteady, incompressible flow (divergence-free velocity field  $\mathbf{u}$ ), governed by the Navier-Stokes (NS) equations,

$$\frac{\partial \mathbf{u}}{\partial t} + (\mathbf{u} \cdot \nabla) \mathbf{u} = - \frac{\nabla p}{\rho_f} + \nu \Delta \mathbf{u}. \quad (11)$$

The Reynolds number,  $Re=(Uw/\nu)$ , which measures the strength of the nonlinear inertial forces to viscous forces, is based on the oscillation velocity ( $U=A\omega$ ), where  $A$  is the oscillation amplitude.  $\nu=\mu/\rho_f$  is the kinematic viscosity. The second, a frequency parameter,  $P_\omega=(U/\omega w)=(A/w)$ , is the ratio of the nonlinear term to the time-derivative term in the NS equations. If the oscillation amplitude  $A$  is small compared to the beam lateral dimension  $w$ ,  $P_\omega$  is small. If  $Re$  and  $P_\omega$  are both small, the nonlinear term is small compared to both viscous and time derivative terms and a solution of the NS equation which neglects the nonlinear term while retaining the time derivative term is appropriate. Stokes' familiar formulas for drag from steady viscous flow around a sphere ( $6\pi\mu Ru$ ) or cylinder are solutions which neglect both the nonlinear term as well as the unsteady term. For typical micro-oscillator frequencies, the velocity gradient generation at the oscillator wall (time scale  $1/\omega$ ) is faster than can be smoothed by viscosity (time scale  $w^2/4\nu$ ) and the unsteady term may not be neglected. The steady solution does not account for the frequency dependence of damping and does not correctly represent its variation with beam size and fluid properties.

For long beams with a cross section of aspect ratio near one, we use the unsteady solution for flow around a long cylinder oscillating normal to its axis, also due to Stokes, discussed in Rosenhead [13]. This solution is presented in terms of two dimensionless parameters  $\kappa_c$  for fluid damping and  $\kappa_m$  for fluid added mass. They are calculated in terms of modified Bessel functions involving a single dimensionless parameter  $\beta$ , which measures the strength of the time derivative term with respect to the viscous term.  $\beta$  is related to familiar physical quantities through

$$\beta=(\omega w^2/4\nu)=0.5(w/\delta)^2=(Re/4P_\omega), \quad (12)$$

where  $\delta=\sqrt{2\nu/\omega}$  measures the viscous layer thickness. To avoid ambiguities in selecting the correct Bessel functions, we present in Ref. [14], six lines of code for the commonly available software program MATLAB, which enables calculation of  $\kappa_c$  and  $\kappa_m$ , based on a more convenient equivalent expression for the solution [3]. The fluid damping coefficient  $C_f$  we require is related to  $\kappa_c$  through

$$C_f=\pi\mu l\beta\kappa_c. \quad (13)$$

For a fixed dynamic viscosity  $\mu=\nu\rho_f$ , the dimensionless product  $\beta\kappa_c$  specifies the dependence of fluid damping on beam width, oscillation frequency and fluid density. It is plotted in Fig. 3. When the viscous layer thickness is much larger than beam size, it approaches the constant value of 1.1 from the quasisteady Stokes solution for a long beam ( $l/w=20$ ). It increases rapidly with decreasing viscous layer thicknesses below beam width ( $\delta/w<1$ ), showing that large errors will result from using Stokes' steady solution for damping in this range. For example, Fig. 2 shows the pressure and damping value ranges associated with continuum flow for two beams. In this range, for the  $w=100$  nm,  $L=2$   $\mu$ m beam, frequency 500 MHz,  $\delta/w$  varies from 0.77 to 0.24 and from Fig. 3, nondimensional damping varies from 4.5 to 10 times the quasisteady value. For the  $w=10$   $\mu$ m,

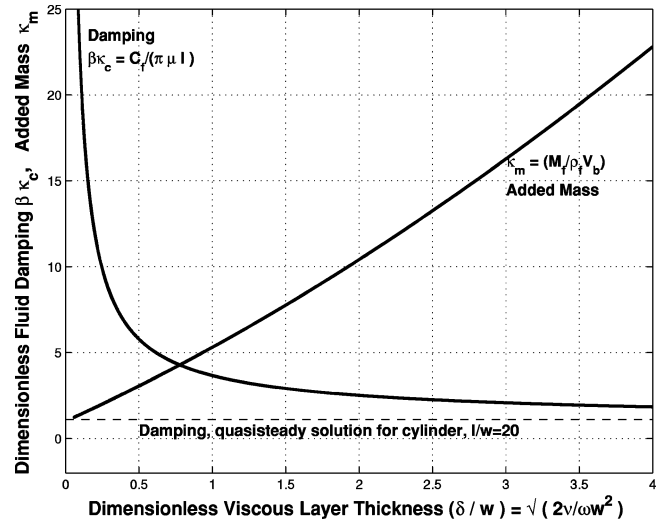


FIG. 3. Unsteady NS solution for fluid damping and added mass for a long cylinder in continuum flow, valid for liquids and for gases with  $Kn<0.01$ .

$L=200$   $\mu$ m beam, with a frequency of 1 MHz,  $\delta/w$  varies from 0.38 to 0.05 and nondimensional damping varies from 7 to 40 times the quasisteady value. This shows that for typical micrometer and nanometer scale beams, at pressures within the continuum range,  $\delta/w<1$ , and we can have a large contribution from unsteady effects. The jump discontinuity at the crossover-continuum interface in Fig. 2 arises from the fact that for these oscillators, while higher damping due to unsteady effects is correctly captured by the continuum solution, all available crossover solutions are restricted to steady flow and hence approach the quasisteady Stokes solution at the continuum end. Development of solutions which include the effects of unsteadiness would be of value to accurate calculations for oscillators in this regime.

Rewriting Eq. (13) using Eq. (6) for viscosity, damping

$$C_f=[1.41\beta\kappa_c Kn]mnU_{th}wl \quad (14)$$

shows a linear dependence on  $Kn$ , consistent with the crossover solution. We have shown that fluid damping  $C_f$  in a gaseous environment for the beam in all flow regimes is proportional to  $(mnU_{th}wl)$ . We have specified how the proportionality constants or dimensionless groups may be calculated from beam geometry, oscillation frequency and gas molecular weight, pressure, and temperature for each of the three regimes. In liquids, the kinematic viscosity, beam size, and frequency may be used with Eq. (12) and Ref. [14] to determine fluid damping. The value of  $C_f$  is used in Eq. (4) to calculate the quality factor  $Q_p$ . Effective damping  $C=C_s+C_f$  is used in Eq. (2) to check the frequency change due to fluid damping.

In the continuum regime where added mass effects may be significant, the modification to  $Q_p$  due to fluid added mass in Eq. (4) is the factor

$$R_m=(1+M_f/M_s)^{1/2}=\left(1+\frac{\rho_f}{\rho_s}\kappa_m\right)^{1/2}, \quad (15)$$

and the effective mass,  $M = M_s R_m^2$ , may be used in Eq. (2) to check the frequency change due to fluid added mass. The factor  $R_m$  is governed by two dimensionless parameters, the ratio of fluid to solid density, and  $\kappa_m$ , which specifies, through  $\beta$ , the fluid added mass dependency on kinematic viscosity, oscillation frequency and beam width.  $\kappa_m$ , calculated as in Ref. [14], is plotted in Fig. 3. It reduces to the inviscid limit of 1 as the kinematic viscosity becomes small. For dry  $N_2$  at 10 atm and 300 K, and for the beams in Fig. 2,  $R_m$  is 1.007, 1.005, making the effective mass 1.4 and 1% higher than beam solid mass  $M_s$ , for the 0.1 and 10  $\mu\text{m}$  beams, respectively. For the same beams in water the factor  $R_m$  is 1.46, 1.32 with beam effective mass 2.1, 1.7 times  $M_s$  and in mercury,  $R_m$  is 3.14, 2.86, with beam effective mass 9.9, 8.2 times  $M_s$ .

The resulting variation of  $Q$  factor with pressure in dry nitrogen is plotted in Fig. 4 for two beams and is seen to be in accord with available experimental data. The values for  $Q$  in vacuum have been taken from experimental data [1,2]. The pressure limit below which fluid damping causes a negligible decrease in the  $Q$  factor is 1 mtorr for a 10  $\mu\text{m}$  wide cantilever beam and about 1 torr for the 100 nm wide beam. This limit depends on the fluid, beam size, and value of  $Q$  in vacuum (or  $C_s$ ) and may be calculated as shown here.

In vacuum, the larger beam with higher surface to volume has a higher  $Q$  factor. But in the presence of air, as the pressure is increased, the  $Q$  factor of the larger beam begins to decrease at an earlier pressure. This results in a reversal, with the  $Q$  factor of the smaller beam being over an order of magnitude higher than that of the larger beam. This reversal of the  $Q$  factor at low pressure is due to the fact that damping varies linearly with width in the free molecular regime. In the continuum regime, it is sustained by the unsteady effects on damping. The width-dependence of damping ( $\beta\kappa_c$ ) from the unsteady solution is not seen in the quasisteady Stokes solution.

These results are particularly interesting for instrument design as they suggest that moving to submicrometer-sized

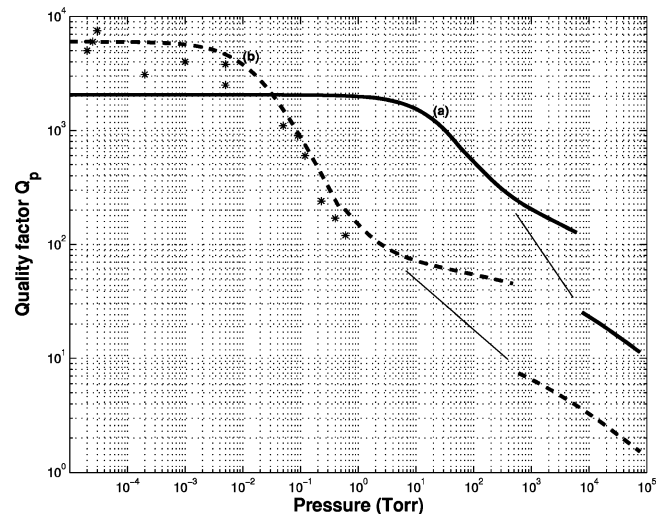


FIG. 4. Calculated  $Q$  factor as a function of pressure in dry nitrogen at 300 K, for beams with aspect ratio  $l/w = 20$  and (a)  $w = 100$  nm, 530 MHz frequency, doubly clamped beam (solid line) (b)  $w = 10$   $\mu\text{m}$ , 85 kHz frequency, cantilever beam (dashed line). Experimental data (\*) are from Fig. 4 of Yasumura *et al.* [15]. A more complete unsteady Boltzmann solution, currently unavailable to the authors, would remove the jump discontinuity at the crossover-continuum interface, as roughly indicated by the light solid lines.

oscillators should significantly improve the  $Q$  factor when constrained to work in air. Over a large range of pressures, long beams of several micrometers width suffer seriously from air damping while submicrometer scale beams do not.

We acknowledge the financial support of the NSF through the Cornell Center for Materials Research. We wish to thank L. Sekaric for an introduction to the problem, Harold Craighead for his strong support and encouragement of this work, D. Koch and J. Parpia for insightful questions and discussion and M. Foquet for useful comments on a draft of the manuscript.

- 
- [1] D.W. Carr, S. Evoy, L. Sekaric, H.G. Craighead, and J.M. Parpia, *Appl. Phys. Lett.* **75**, 920 (1999).
- [2] K.Y. Yasumura, T.D. Stowe, E.M. Chow, T. Pfafman, T.W. Kenny, B.C. Stipe, and D. Rugar, *J. MEMS* **9**, 117 (2000).
- [3] J.E. Sader, *J. Appl. Phys.* **84**, 64 (1998).
- [4] C-M. Ho and Y-C. Tai, *Ann. Rev. Fluid Mech.* **30**, 579 (1998).
- [5] B. Ilic, D. Czaplowski, M. Zalalutdinov, H.G. Craighead, P. Neuzil, C. Campagnolo, and C. Batt, *J. Vac. Sci. Technol. B* **19**, 2825 (2001).
- [6] L. Sekaric, M. Zalalutdinov, R.B. Bhiladvala, A.T. Zehnder, J.M. Parpia, and H.G. Craighead, *Appl. Phys. Lett.* **81**, 2641 (2002).
- [7] T. Naik, E.K. Longmire, and S.C. Mantell, *Sens. Actuators A* **102**, 240 (2003).
- [8] G. Li and H. Hughes, *Proc. SPIE* **4176**, 30 (2000).
- [9] F. Reif, *Fundamentals of Statistical and Thermal Physics* (McGraw Hill, New York, 1965).
- [10] G.E. Karniadakis and A. Beskok, *Microflows* (Springer-Verlag, New York, 2002).
- [11] G.N. Patterson, *Molecular Flow of Gases* (Wiley, New York, 1956).
- [12] K. Yamamoto and K. Sera, *Phys. Fluids* **28**, 1286 (1985).
- [13] L. Rosenhead, *Laminar Boundary Layers* (■, Oxford, 1963), Sec. VII.12.
- [14]  $z = -i * \text{sqrt}(i) * \text{sqrt}(\beta); K1 = \text{besselk}(1, z); K0 = \text{besselk}(0, z); FK1 = 1 + (4 * K1) ./ (z * K0); K_m = \text{real}(FK1); K_c = \text{imag}(FK1)$ .
- [15] Figure 4 in Ref. [2] does not quote other dimensions for this 510 nm thick cantilever. Using their Fig. 5, we have assumed  $w = 10$   $\mu\text{m}$ ,  $l = 200$   $\mu\text{m}$  (midrange) for this rough comparison, as no comparable experimental data are known to the authors.